Electron tomography of (In,Ga)N insertions in GaN nanocolumns grown on semi-polar (11 2¯2) GaN templates

M. Niehle, A. Trampert, S. Albert, A. Bengoechea-Encabo, and E. Calleja

Citation: APL Materials **3**, 036102 (2015); doi: 10.1063/1.4914102
View online: http://dx.doi.org/10.1063/1.4914102
View Table of Contents: http://scitation.aip.org/content/aip/journal/aplmater/3/3?ver=pdfcov
Published by the AIP Publishing

APL MATERIALS **3**, 036102 (2015)

Electron tomography of (In,Ga)N insertions in GaN nanocolumns grown on semi-polar (11$\bar{2}$2) GaN templates

M. Niehle,[1,a] A. Trampert,[1,b] S. Albert,[2] A. Bengoechea-Encabo,[2] and E. Calleja[2]
[1]*Paul-Drude-Institut für Festkörperelektronik, Hausvogteiplatz 5-7, 10117 Berlin, Germany*
[2]*ISOM and Departamento de Ingeniería Electrónica, ETSI Telecomunicación, Universidad Politécnica de Madrid, Ciudad Universitaria s/n, 28040 Madrid, Spain*

(Received 22 January 2015; accepted 24 February 2015; published online 3 March 2015)

We present results of scanning transmission electron tomography on GaN/(In,Ga)N/GaN nanocolumns (NCs) that grew uniformly inclined towards the patterned, semi-polar GaN(11$\bar{2}$2) substrate surface by molecular beam epitaxy. For the practical realization of the tomographic experiment, the nanocolumn axis has been aligned parallel to the rotation axis of the electron microscope goniometer. The tomographic reconstruction allows for the determination of the three-dimensional indium distribution inside the nanocolumns. This distribution is strongly interrelated with the nanocolumn morphology and faceting. The (In,Ga)N layer thickness and the indium concentration differ between crystallographically equivalent and non-equivalent facets. The largest thickness and the highest indium concentration are found at the nanocolumn apex parallel to the basal planes. [http://dx.doi.org/10.1063/1.4914102]

Semiconductor nanowires and nanocolumns (NCs) are discussed in the literature as potential building blocks for the fabrication of future nano-scaled optoelectronic or photovoltaic devices. A crucial prerequisite is, however, a precise control on their three-dimensional geometry, shape, and composition. Selective area growth (SAG) of nanowires and -columns has been proven as a promising technique to achieve these requirements.[1] Accordingly, the SAG by molecular beam epitaxy on patterned substrates has demonstrated the successful realization of well-ordered arrays of GaN NCs including homogeneous axial (In,Ga)N/GaN heterostructures.[2] Furthermore, the selection of the interface orientation is crucial. The growth of (In,Ga)N on non- or semi-polar facets is pursued to circumvent the consequences of strong internal electric fields along the polar ⟨0001⟩ direction of the GaN wurtzite structure.[3] The major approaches suggest using either a corresponding substrate orientation[4,5] or radial NC heterostructures with preferential incorporation of indium on the side-facet of the NCs grown on polar substrates.[6,7] The microstructure and local chemical composition of those perfectly aligned NCs can be analyzed by high-resolution and analytical transmission electron microscopy (TEM). As long as the one-dimensional (1D) nanostructures reflect a high symmetry with respect to the substrate and along the growth direction, standard plan-view and cross-sectional TEM investigations are sufficiently applicable.[8] On the other hand, a higher complexity in the NC geometry as well as in the internal structure demands a more complete three-dimensional structural and chemical information that cannot be extracted from various TEM projections only. Here, electron tomography has been recently applied to measure for instance the variations in surface morphology[9,10] or the three-dimensional distribution of the electrostatic potential in III-V nanowires.[11] In this report, the complex morphology of ordered (In,Ga)N/GaN NCs inclined to the substrate and the spatial elemental distribution of indium is disclosed by scanning

[a]niehle@pdi-berlin.de
[b]trampert@pdi-berlin.de

transmission electron tomography which tackles the challenge of the three-dimensional problem on the nanometer scale. The tomography conclusively reveals a core-shell like GaN/(In,Ga)N/GaN heterostructure of the columns with a (In,Ga)N insertion along the c-plane close to the apex.

The investigated NCs have been grown on a semi-polar $(11\bar{2}2)$ GaN template (fabricated on a $(1\bar{1}00)$ Al_2O_3 substrate) by molecular beam epitaxy (MBE). The growth started with a GaN deposition for 3 h followed by the deposition of (In,Ga)N for 160 s. A final step of GaN growth for 5 min has been applied to cap the (In,Ga)N. The SAG process proceeded on a Ti nanomask deposited onto the substrate.[4] The preferential growth direction is found to be perpendicular to the c-plane, what forces an inclined growth of the NCs in respect to the substrate (see Fig. 1).[5] Growth details are described in the publication of Bengoechea-Encabo *et al.*[5] The scanning electron microscopy (SEM) images in Fig. 1(a) along the $[000\bar{1}]$ direction and (b) in a bird's eye view along with the scheme in Fig. 1(c) illustrate the geometric situation. The NCs are homogeneously inclined with their axis toward the sample surface due to the preferred growth along the [0001] direction. The SEM image in Fig. 1(a) depicts the hexagonal symmetry of the bordering faces around the [0001] axis. The orientation relationship between the $(11\bar{2}2)$ surface and the [0001] direction is illustrated in Fig. 1(c) along with the morphological notion from the SEM results. The angle between the basal and the surface plane amounts to 58.4°.

The investigation of the (In,Ga)N insertions by electron tomography necessitates to fit the specimen geometry to the NCs and to select an adequate imaging mode. The first prerequisite is realized with a focused ion beam (FIB) integrated in a dual-beam microscope (JEOL IB4501) equipped with a versatile sample stage and a micro-manipulator (Kleindiek). The sample is mounted on a tomography holder (Fischione model 2050) with its [0001] direction approximately aligned to the TEM goniometer tilt axis (cf. Fig. 2). This geometric condition allows to minimize the thickness that has to be transmitted by electrons and enables imaging along the low indexed $\langle 1\bar{1}00\rangle$ and $\langle 11\bar{2}0\rangle$ directions in contrast to conventionally prepared cross-section samples which only allow the imaging along the low indexed $[1\bar{1}00]$ or $[\bar{1}100]$ direction as shown in Fig. 1(d). The challenge to machine GaN with a gallium ion beam and isolating Al_2O_3 with a charged particle beam in general has to be noted at this point.

The second requirement is met by the selection of scanning transmission electron microscopy (STEM) imaging using the high-angle annular dark-field (HAADF) signal. HAADF STEM contrast

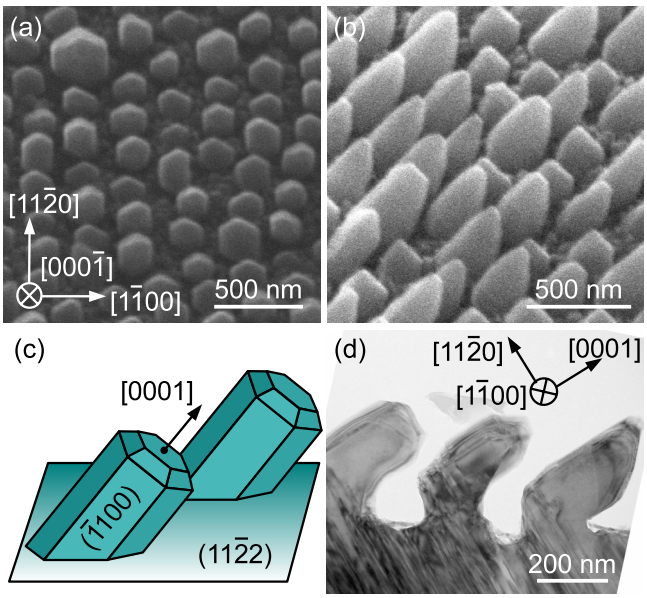

FIG. 1. SEM images (a) and (b) show the hexagonal shape and the homogeneous inclination of GaN/(In,Ga)N NCs, respectively. The schematic (c) illustrates the orientation relation of NCs towards the substrate surface. (d) The CTEM bright-field image of a cross-section sample viewed along the $[1\bar{1}00]$ zone axis is sensitive to defects on basal planes.

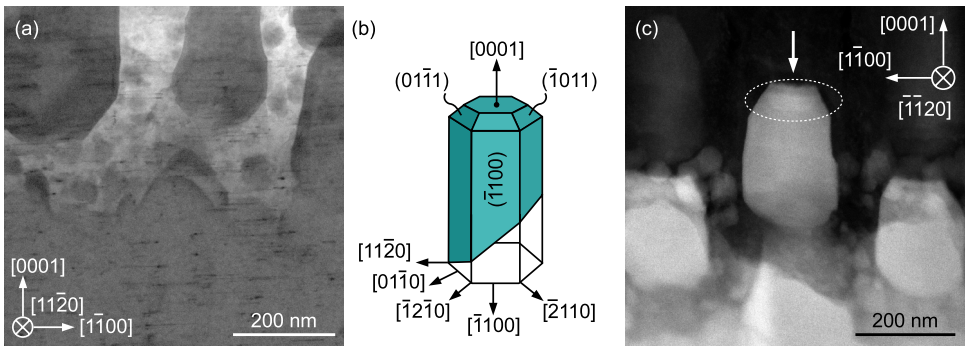

FIG. 2. (a) The bright-field STEM image along the [11$\bar{2}$0] zone axis provides information about defects on basal planes based on diffraction contrast which is suppressed in (c) the HAADF STEM image in the same direction. The latter imaging mode is exploited for its chemical sensitivity to reveal the distribution of (In,Ga)N in the NC marked by an arrow. (b) The scheme depicts the used allocation of crystallographic directions and lattice planes to the analyzed NC.

is dominantly sensitive to the sample thickness and its chemical composition (Fig. 2(c)). In contrast, bright-field images in conventional transmission electron microscopy (CTEM) and STEM mode shown in Figs. 1(d) and 2(a), respectively, are dominated by diffraction contrast. These examples highlight defects parallel to the basal planes and provide complementary information. On the other hand, contrast features perpendicular to the basal planes in Fig. 1(d) are thickness fringes. Furthermore, the monotonic variation of HAADF intensity with thickness is required for the tomography reconstruction which is not fulfilled for diffraction contrast.[12] Therefore, HAADF is the preferred signal for electron tomography in materials science[13] although BF STEM images provide a better signal to noise ratio. STEM and CTEM measurements have been carried out using a JEOL 2100F microscope.

A HAADF tilt-series in steps of 3° from −81° to +84° has been acquired. Figure 2(c) shows one image from this series taken along the [11$\bar{2}$0] direction. The 270 nm thick lamella comprises an ensemble of NCs. The original template surface is inclined to the image plane. Particles at the surface are related to parasitic growth. The NC of interest (marked by an arrow) has little overlap with the template during tilting to reduce the thickness of GaN that has to be penetrated by the electron beam. This is important because the intensity I — as a prerequisite for the tomographic reconstruction — has to linearly increase with thickness t which does not hold for the lamella at the position of the template. Furthermore, the HAADF signal is sensitive to the chemical composition, i.e., $I \propto Z^{1.7}$, where Z is the atomic number.[14] Fig. 2(c) shows, consequently, an (In,Ga)N inclusion or a higher indium concentration, respectively, at the apex of the NC (marked by the dashed ellipse).

The analysis of the spatial distribution of indium is based on the three-dimensionally reconstructed volume from the tilt series and the adequate representation of the volume both realized with the IMOD software package.[15] The visualization of only one intensity value of the reconstructed data set is called an isosurface. The isosurface presentations in Fig. 3 (left column) allow the description of the NC morphology and the facet determination. A rough surface parallel to the (0001) plane is clearly resolved (Figs. 3(b)-3(d)). In contrast, there are smooth and extended {10$\bar{1}$0} side facets and several pyramidal {10$\bar{1}$1} facets that appear near the top and at the bottom of the NC and occasionally as steps interrupting the {10$\bar{1}$0} facets (Fig. 3(d)). Besides, the influence of the inclined growth of the NC and, consequently, the shadowing of one side from the molecular beam is reflected by the non-uniformly developed pyramidal facets. We observe distinct facets of ($\bar{1}$101), (1$\bar{1}$01), ($\bar{1}$011), and (0$\bar{1}$11) type, respectively. The remaining (10$\bar{1}$1) and (01$\bar{1}$1) facets are, however, almost disappeared (see Figs. 3(b) and 3(d)).

The presentation of two isosurface values allows to describe the shape of the (In,Ga)N inclusion with respect to the morphology of the NC. For this purpose, the isosurface of the GaN is presented semitransparent, and the intensity value corresponding to the (In,Ga)N part is added as a red opaque isosurface.[16,17] The different views of this semitransparent isosurface representation in the right column of Fig. 3 reveal the morphology of the (In,Ga)N inclusion and thus verify

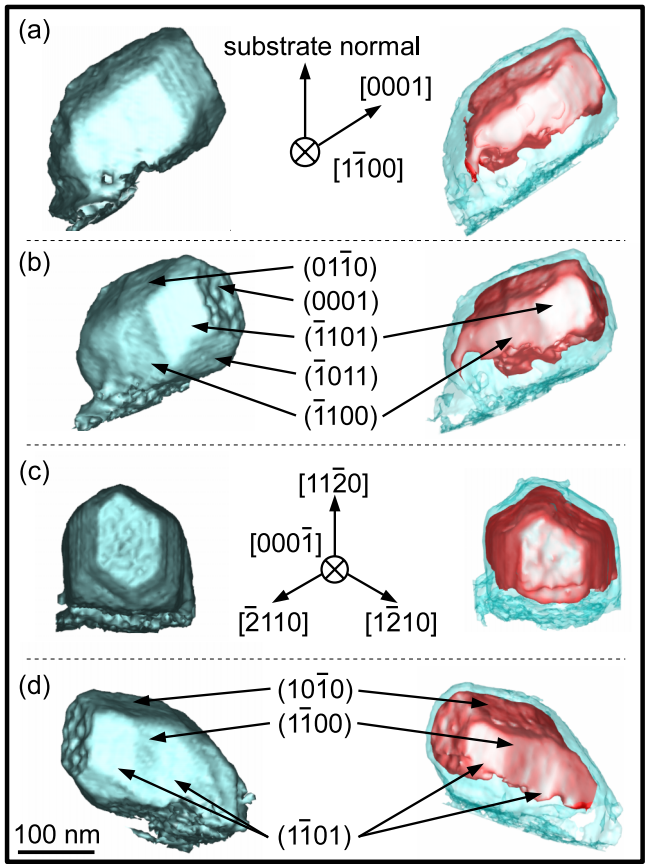

FIG. 3. Isosurface visualization: the opaque representation on the left column illustrates the morphology of the nanoobject. The right column reflects the red opaque (In,Ga)N shell that resembles the outer morphology which is presented semitransparent in this montage of two isosurfaces.

that the (In,Ga)N layers replicate the NC morphology, i.e., they appear as pyramidal and prism planes as well as on the basal plane. Furthermore, it is clearly recognizable that the (In,Ga)N is completely capped by a thin GaN layer. As a consequence, the GaN/(In,Ga)N/GaN NC is arranged as a core-shell like heterostructure with the limitation of being not completely closed at the part inclined to the substrate.

The detailed investigation of the spatial indium distribution is qualitatively analyzed by slices through the reconstructed volume and is summarized in Fig. 4. The positions of the slices are indicated in the isosurface rendered tomograms of the NC shown in the left part of the figure. The lower one is the same as in Fig. 3(c) and the upper one corresponds to the view along the [$\bar{1}\bar{1}$20] direction. The gray values of the reconstructed volume are color coded with red as location of highest average atomic number Z.

Slices 1–3 intersect the NC parallel to the basal planes. The highest indium concentration is found below a thin GaN capping layer near the apex as shown in slices 1 and 2. Red arrows highlight transitions to a lower indium content at the edges. The section through the prism facets in slice 3 reveals the incomplete (In,Ga)N shell with an even lower indium concentration. The next three slices represent sections perpendicular to the {$\bar{1}$100} facets and parallel to the [0001] direction. Slice 4 provides an explanation for the change of the indium concentration in slices 1 and 2: an (In,Ga)N layer with the lower indium content evolves on pyramidal facets and enlarges the basal plane at the apex during growth due to a higher growth rate. Hence, the higher amount of indium incorporated on the basal planes allows to reconstruct the growth front. The distance of the red arrows is consequently larger near the apex. Slices 5 and 6 confirm the presence of the (In,Ga)N shell on prism facets (01$\bar{1}$0) and (10$\bar{1}$0) and the absence on the respective opposite facets. The missing coverage by indium is

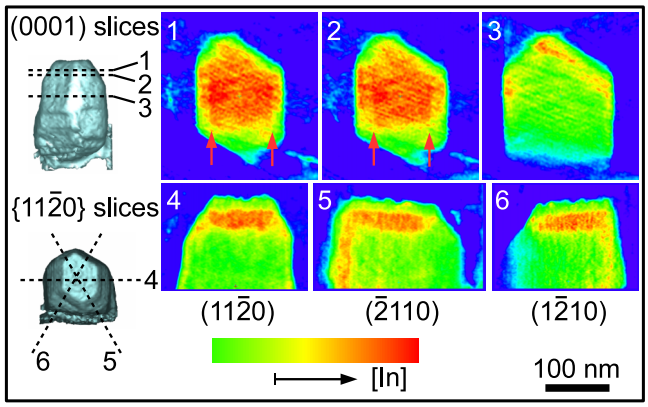

FIG. 4. Slices through the reconstructed volume: the position of the slices 1–6 is marked in the isosurface representations on the left.

considered to be a consequence of the shadowed facets due to their inclination towards the substrate and an insufficient diffusion of indium on the surface during growth.

Our electron tomography results demonstrate the spatial distribution of (In,Ga)N inclusions in GaN NCs resulting in a core-shell like structure. These findings allow to interpret the spatially resolved cathodoluminescence measurements of the NCs[5] and contribute to a more fundamental understanding of the growth mechanisms.

In summary, the qualitative indium distribution in GaN/(In,Ga)N/GaN NC heterostructures is directly observed in the tomography data and, hence, reveals the formerly expected (In,Ga)N insertions.[5] The thickness of the (In,Ga)N insertions and the spatial indium distribution is strongly related to the NCs morphology. The incorporation of indium depends on the crystallographically different lattice planes. Furthermore, the particular geometry of the NCs with respect to the substrate leads to unequal thicknesses of the (In,Ga)N layers parallel to crystallographically equivalent lattice planes. Eventually, the (In,Ga)N does not form a closed shell around the NC. All these results on complex 3D structures and their spatial chemical element distribution are uniquely accessible by electron tomography in combination with an advanced sample preparation method based on FIB.

We thank Stefan Fölsch for critical reading of the manuscript.

[1] H. Sekiguchi, K. Kishino, and A. Kikuchi, Appl. Phys. Express **1**, 124002 (2008).
[2] S. Albert, A. Bengoechea-Encabo, P. Lefebvre, F. Barbagini, M. Sanchez-Garcia, E. Calleja, U. Jahn, and A. Trampert, Appl. Phys. Lett. **100**, 231906 (2012).
[3] S. Li and A. Waag, J. Appl. Phys. **111**, 071101 (2012).
[4] A. Bengoechea-Encabo, S. Albert, M. S. García, L. López, S. Estradé, J. Rebled, F. Peiró, G. Nataf, P. de Mierry, J. Zuniga-Perez, and E. Calleja, J. Cryst. Growth **353**, 1 (2012).
[5] A. Bengoechea-Encabo, S. Albert, J. Zuñiga-Perez, P. de Mierry, A. Trampert, F. Barbagini, M. A. Sanchez-Garcia, and E. Calleja, Appl. Phys. Lett. **103**, 241905 (2013).
[6] T.-W. Yeh, Y.-T. Lin, L. Stewart, P. Dapkus, R. Sarkissian, J. O'Brien, B. Ahn, and S. Nutt, Nano Lett. **12**, 3257 (2012).
[7] J. Grandal, M. Wu, X. Kong, E. Dimakis, M. Hanke, L. Geelhaar, H. Riechert, and A. Trampert, Appl. Phys. Lett. **105**, 121602 (2014).
[8] A. Trampert, X. Kong, E. Luna, J. Grandal, and B. Jenichen, "Microstructure of group III-N nanowires," in *Wide Band Gap Semiconductor Nanowires 1* (John Wiley & Sons, Inc., 2014), pp. 125–156.
[9] H. Kim, Y. Myung, Y. Cho, D. M. Jang, C. Jung, and J. Park, Nano Lett. **10**, 1682 (2010).
[10] M. Verheijen, R. E. Algra, M. Borgström, G. Immink, E. Sourty, W. van Enckevort, E. Vlieg, and E. Bakkers, Nano Lett. **7**, 3051 (2007).
[11] D. Wolf, H. Lichte, G. Pozzi, P. Prete, and N. Lovergine, Appl. Phys. Lett. **98**, 264103 (2011).
[12] H. Friedrich, M. McCartney, and P. Buseck, Ultramicroscopy **106**, 18 (2005).
[13] P. Midgley and M. Weyland, Ultramicroscopy **96**, 413 (2003).
[14] P. Hartel, H. Rose, and C. Dinges, Ultramicroscopy **63**, 93 (1996).
[15] J. Kremer, D. Mastronarde, and J. McIntosh, J. Struct. Biol. **116**, 71 (1996).
[16] The selected intensity value can only represent (In,Ga)N with one fixed indium concentration. We have chosen in Fig. 3 a value that visualizes (In,Ga)N with the lowest detectable indium content. Abrupt intensity changes at interfaces in STEM images are slightly smeared out in the reconstructed 3D data set.[17] As a consequence, the shape of regions with higher indium content compared to the selected value is, therefore, inherently included in the isosurface representation.
[17] J.-J. Fernandez, Micron **43**, 1010 (2012).